

Supplementary Information for

Integrated optical parametric amplifiers in silicon nitride waveguides incorporated with 2D graphene oxide films

Yang Qu^{1,#}, Jiayang Wu^{1,#,}, Yuning Zhang¹, Yunyi Yang¹, Linnan Jia¹, Houssein El Dirani²,
[+], Sébastien Kerdiles², Corrado Sciancalepore^{2, [++]}, Pierre Demongodin³, Christian Grillet³,
Christelle Monat³, Baohua Jia^{4,5,*}, and David J. Moss^{1,*}*

¹Optical Sciences Centre, Swinburne University of Technology, Hawthorn, VIC 3122, Australia

²Université Grenoble-Alpes, CEA-LETI, 17 Avenue des Martyrs, 38054 Grenoble, France

[+]Current address: LIGENEC SA, 224 Bd John Kennedy, 91100 Corbeil-Essonnes, France

[++]Current address: Soitec SA, 38190 Bernin, France

³Université de Lyon, Ecole Centrale de Lyon, INSA Lyon, Université Claude Bernard Lyon 1, CPE Lyon, CNRS, INL, UMR5270, 69130 Ecully, France

⁴Centre for Atomaterials and Nanomanufacturing, School of Science, RMIT University, Melbourne, VIC 3000, Australia

⁵Australian Research Council (ARC) Industrial Transformation Training, Centre in Surface Engineering for Advanced Materials (SEAM), RMIT University, Melbourne, Victoria 3000, Australia

#These authors contribute equally.

*E-mail: jiayangwu@swin.edu.au, baohua.jia@rmit.edu.au, dmoss@swin.edu.au

Number of pages: 12

Number of Figures: 7

This supplementary information includes the following sections:

- I. Experimental setup for loss measurements**
- II. OPA experiments using a picosecond pulsed pump**
- III. Fitting OPA experiments with theory**
- IV. Improving OPA performance by simultaneously optimizing multiple parameters**
- V. Optimizing OPA performance by changing the coating position of GO film**
- VI. Influence of GO's saturable absorption (SA) on the OPA performance**

I. Experimental setup for loss measurements

We used the experimental setup shown in **Figure S1** to characterize the linear and nonlinear loss of the fabricated devices. Two different laser sources were employed, including a tunable continuous-wave (CW) laser and a femtosecond fiber pulsed laser (FPL) used for linear and nonlinear loss measurements, respectively. The light was coupled to the device under test (DUT) using lensed fibers butt coupled to inverse-taper couplers at both ends of the waveguides. To achieve TE-polarization, a polarization controller (PC) was utilized to adjust the polarization of the input light. The average power was measured before and after the DUT using optical power meters (OPM 1 and OPM 2). A broadband variable optical attenuator (VOA) was used to adjust the input power, and to prevent damage to the laser, a broadband optical isolator was inserted. The femtosecond optical pulses generated by the FPL were nearly Fourier-transform limited [1, 2], with a pulse duration of ~ 180 fs and a repetition rate of ~ 60 MHz.

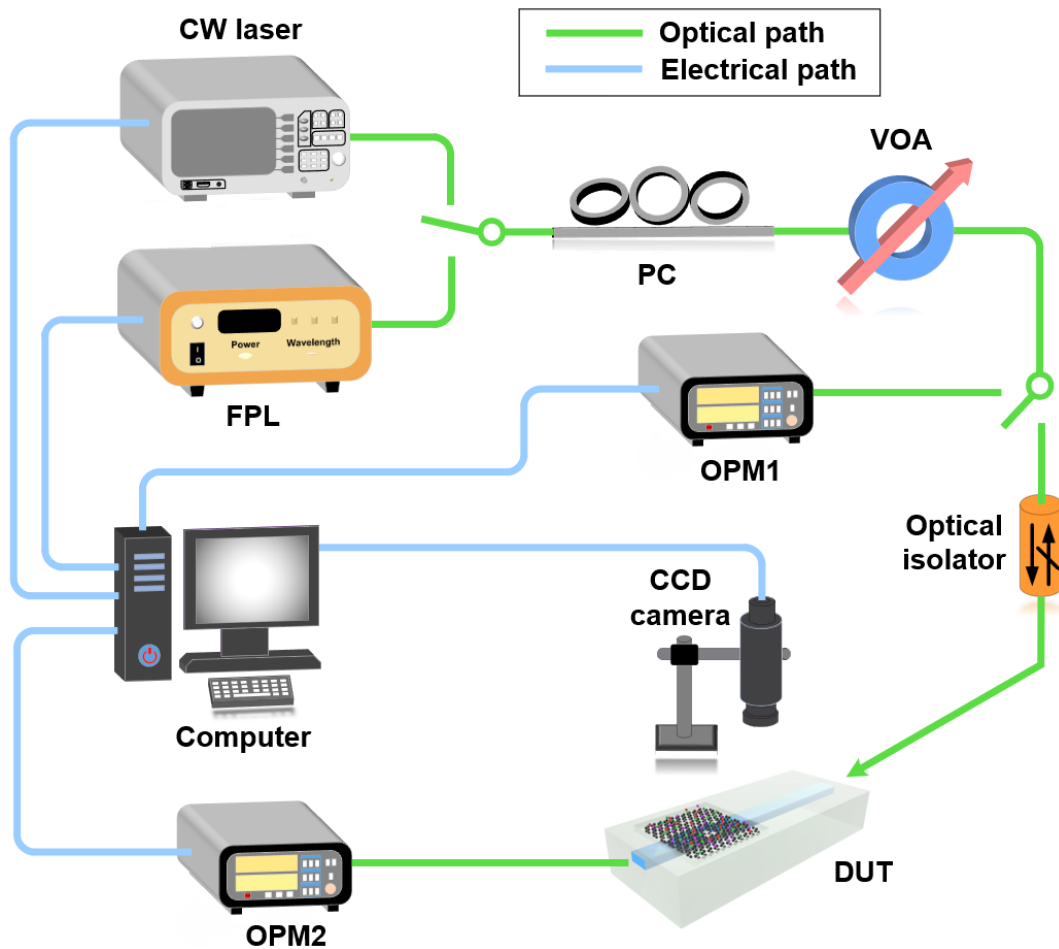


Figure S1. Experimental setup for loss measurements. CW laser: continuous-wave laser. FPL: fiber pulsed laser. PC: polarization controller. EDFA: erbium doped fiber amplifier. VOA: variable optical attenuator. OPM: optical power meter. DUT: device under test. CCD: charged-coupled device.

II. OPA experiments using a picosecond pulsed pump

In addition to using femtosecond optical pulses as the pump, we also employ picosecond optical pulses generated by another fiber pulsed laser to perform OPA experiments. The picosecond optical pulses have a pulse width of ~ 2.0 ps and a maximum peak power of ~ 60 W.

Figure S2a shows the optical spectra after propagation through the uncoated Si_3N_4 waveguide and the hybrid waveguides with 1 and 2 layers of GO. For all three devices, the input pump peak power and signal power are kept the same at $P_{peak} = \sim 60$ W and $P_{signal} = \sim 6$ mW, respectively. **Figure S2b** shows the measured output optical spectra after propagation through the device with 2 layers of GO at different P_{peak} . **Figure S2c** shows the extracted signal parametric gain PG and parametric gain improvement ΔPG versus input pump peak power P_{peak} . As with the OPA experiments that used femtosecond optical pulses as the pump, we noted that the hybrid waveguide with 1 layer of GO showed higher values for both PG and ΔPG than the uncoated waveguide, but lower values than the device with 2 layers of GO. By fitting the experimental results in **Figure S2c** with theory [3-5], we obtained the nonlinear parameter γ 's for the hybrid waveguides. The fit values of γ for devices with 1 and 2 layers of GO were ~ 14.3 and ~ 27.0 times higher, respectively, than the value obtained for the uncoated Si_3N_4 waveguide. These values were similar to the ones shown in **Figure 6a**, which were obtained by fitting experimental results using femtosecond pulsed pump. These results further confirm the improved OPA performance in the hybrid waveguide incorporating 2D GO films.

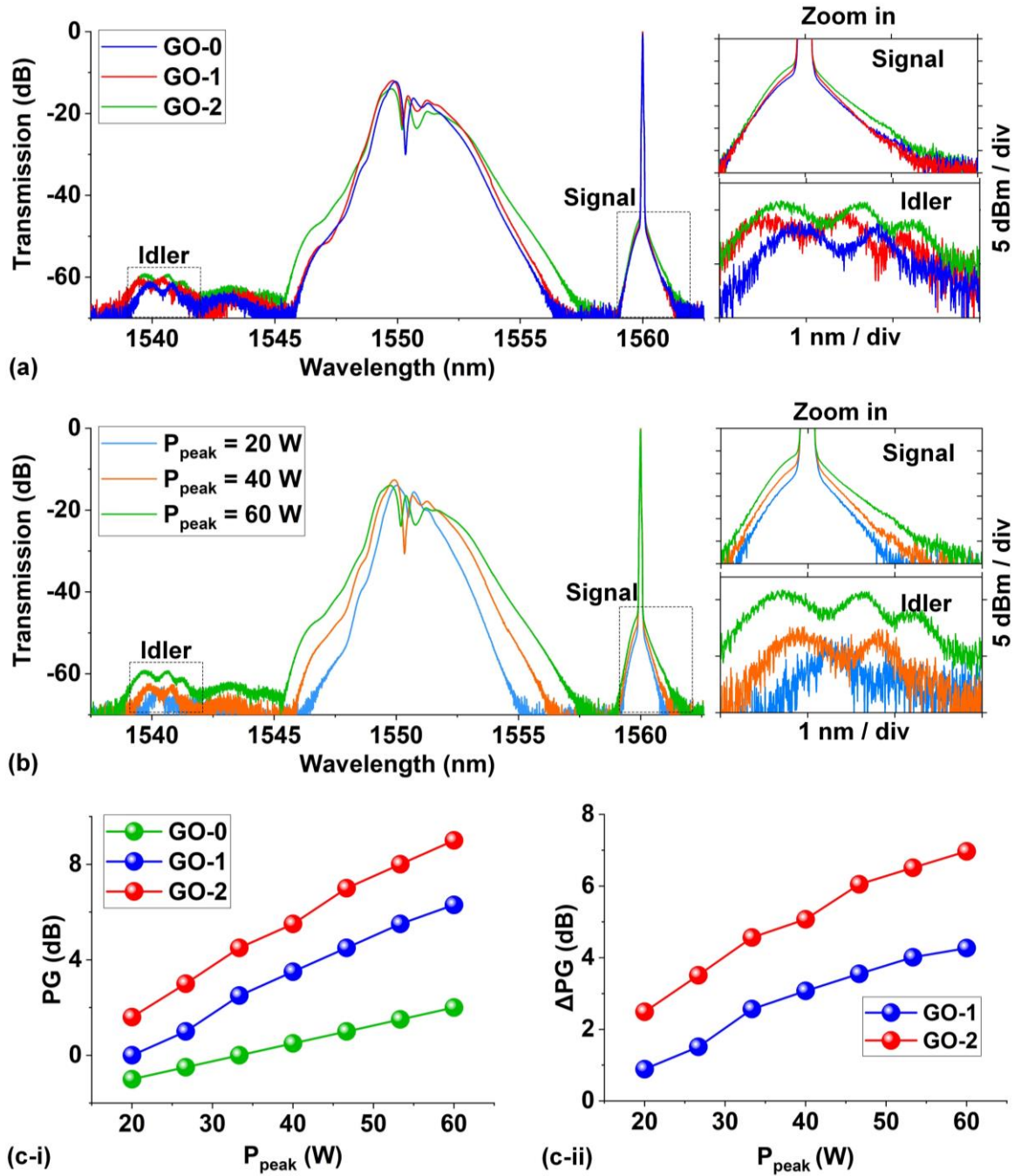


Figure S2. Optical parametric amplification (OPA) using a 3.7-ps pulsed pump and a continuous-wave (CW) signal. (a) Measured output optical spectra after propagation through uncoated (GO-0) and hybrid waveguides with 1 (GO-1) and 2 (GO-2) layers of GO. The peak power of the input pump light P_{peak} is ~ 90 W. (b) Measured output optical spectra after propagation through the device with 2 layers of GO at different P_{peak} . In (a) and (b), the power of the CW signal light is $P_{signal} = \sim 6$ mW, and insets show zoom-in views around the signal and idler. (c) Measured (i) parametric gain PG and (ii) parametric gain improvement ΔPG versus P_{peak} .

III. Fitting OPA experiments with theory

We used the modeling method introduced in [Methods](#) to fit the OPA experiments with theory. Figure S3a shows the measured (data points) and fit (dashed curves) parametric gain PG and parametric gain improvement ΔPG versus pump peak power P_{peak} . The dashed curves were calculated based on the fit result at $P_{peak} = 180$ W. The experimental data points closely match the simulation curves, confirming the consistency between our experimental results and the theoretical predictions. This consistency was also observed in [Figure S3b](#), where we plot the measured parametric gain PG and parametric gain improvement ΔPG versus CW signal power P_{signal} , along with the fit dashed curves at $P_{signal} = 6$ mW. The agreement between the data points and the curves further supports the validity of our experimental and theoretical approaches.

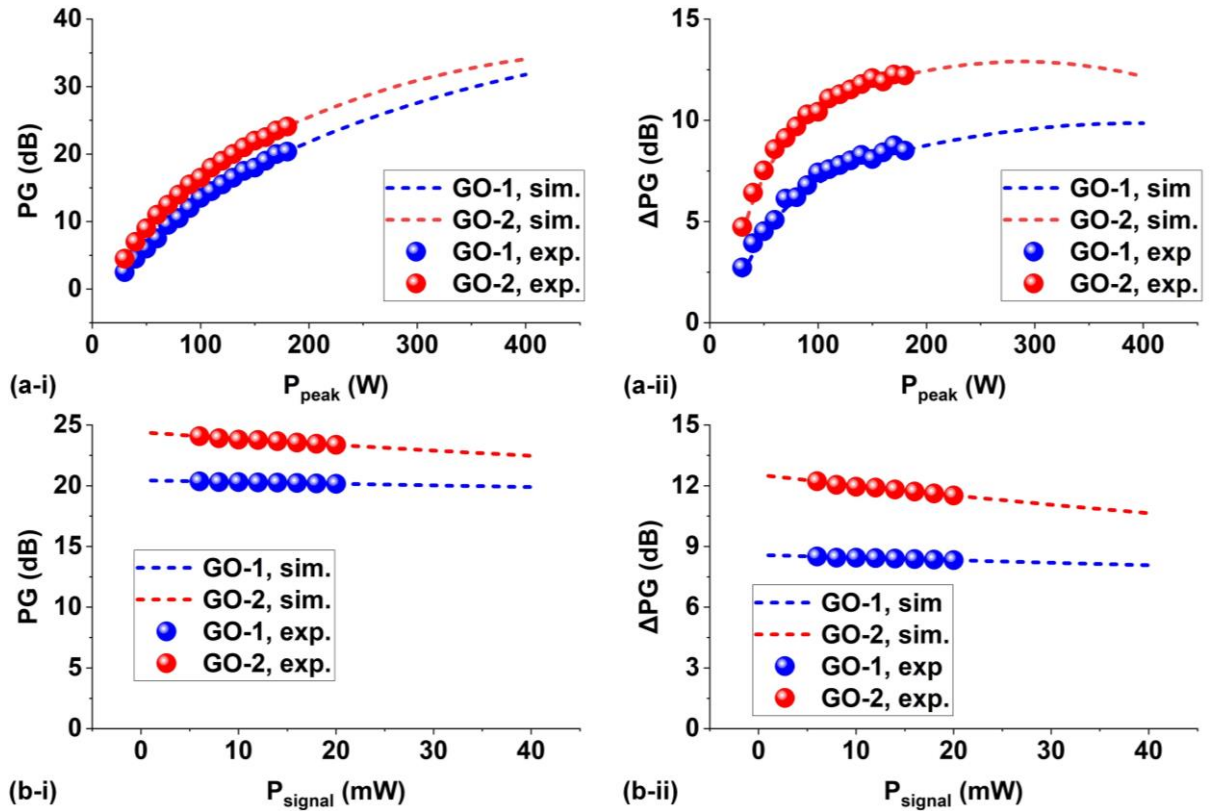


Figure S3. (a) Measured and fit (i) parametric gain PG and (ii) parametric gain improvement ΔPG versus pump peak power P_{peak} . (b) Measured and fit (i) PG and (ii) ΔPG versus CW signal power P_{signal} . In (a) and (b), the measured and fit results are shown by the data points and the dashed curves, respectively. The wavelength detuning and the GO film length are $\Delta\lambda = -22$ nm and $L_{GO} = 1.4$ mm, respectively. In (a), $P_{signal} = 6$ mW. In (b), $P_{peak} = 180$ W.

IV. Improving OPA performance by simultaneously optimizing multiple parameters

Figure S4a shows the calculated PG for the hybrid waveguides versus wavelength detuning $\Delta\lambda$ and GO film length L_{GO} at $P_{peak} = 180$ W. The corresponding results for ΔPG are shown in **Figure S4b**. In each figure, (i) and (ii) show the results for the devices with 1 and 2 layers of GO, respectively. The black points mark the experimental results in **Figure 4**, and the black crossings mark the results corresponding to the maximum values of PG and ΔPG . For the device with 1 layer of GO, the maximum PG of ~ 37.4 dB and ΔPG of ~ 31.5 dB are achieved. Whereas for the device with 2 layers of GO, the maximum PG and ΔPG are ~ 37.8 dB and ~ 27.3 dB, respectively. These values obtained by optimizing both $\Delta\lambda$ and L_{GO} are higher than those obtained by optimizing either $\Delta\lambda$ or L_{GO} alone (as shown in **Figure 8**), indicating the potential for further enhancement.

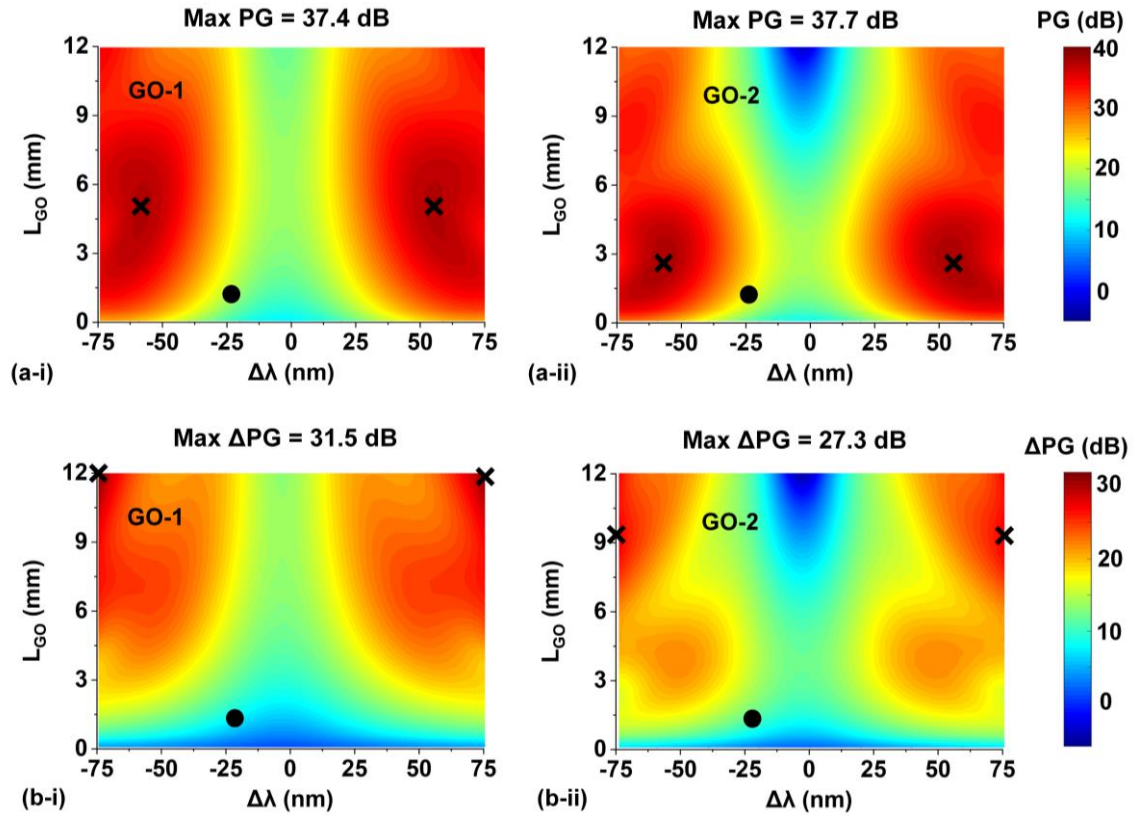


Figure S4. Simulated results for pump peak power $P_{peak} = 180$ W. (a) Simulated parametric gain PG versus wavelength detuning $\Delta\lambda$ and GO film length L_{GO} . (b) Simulated parametric gain improvement ΔPG versus $\Delta\lambda$ and L_{GO} . In (a) and (b), (i) and (ii) show the results for the hybrid waveguides with 1 and 2 layers of GO (GO-1 and GO-2), respectively. The black points mark the OPA experimental results, and the black crossing mark the results corresponding to the maximum values of PG and ΔPG . The signal power is $P_{signal} = 6$ mW.

Figure 5 shows the calculated PG for the hybrid waveguides versus wavelength detuning $\Delta\lambda$ and GO film length L_{GO} at $P_{peak} = 400$ W. The black crossings mark the results corresponding to the maximum values of PG and ΔPG . As can be seen, increasing the pump peak power from 180 W to 400 W can result in even higher maximum PG and ΔPG for the device with 1 layer of GO, with values reaching ~ 43.7 dB and ~ 40.1 dB, respectively. Likewise, the device with 2 layers of GO can achieve a maximum PG of ~ 43.8 dB and a maximum ΔPG of ~ 37.3 dB at $P_{peak} = 400$ W.

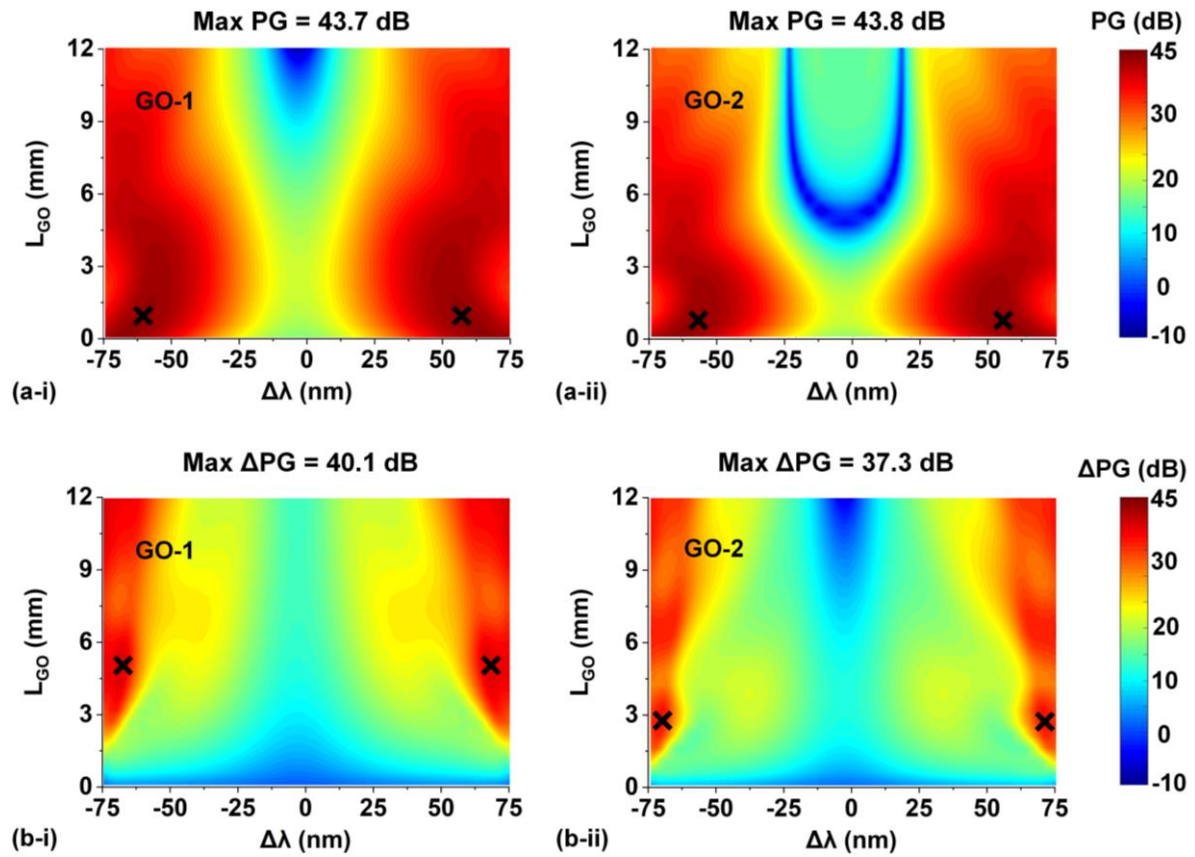


Figure S5. Simulations for pump peak power $P_{peak} = 400$ W. (a) Simulated parametric gain PG versus wavelength detuning $\Delta\lambda$ and GO film length L_{GO} . (b) Simulated parametric gain improvement ΔPG versus $\Delta\lambda$ and L_{GO} . In (a) and (b), (i) and (ii) show the results for the hybrid waveguides with 1 and 2 layers of GO (GO-1 and GO-2), respectively. The black crossing mark the results corresponding to the maximum values of PG and ΔPG . The signal power is $P_{signal} = 6$ mW.

V. Optimizing OPA performance by changing the coating position of GO film

Figures S5a and **S5b** show the calculated PG and ΔPG versus GO coating position L_0 , respectively. The coating position is defined as the distance from the waveguide input port. The dashed curves were calculated based on the fit result at $L_0 = 0.7$ mm marked by the data points. The maximum PG and ΔPG are achieved at $L_0 = 0$ mm, where the pulse peak power is the highest. As L_0 increases, both PG and ΔPG exhibit a non-monotonic behavior, decreasing first and then increasing. This behavior is distinct from the monotonic decrease in spectral broadening induced by self-phase modulation as L_0 increases [6, 7], and can be attributed to the delicate balance between the decrease in pump power and the increase in signal power during the OPA process. To further illustrate this point, we present the evolution of PG with respect to the propagation distance for different L_0 in **Figure S5c**. It is worth noting that although optimizing L_0 yields improvements in PG and ΔPG , these improvements are not as significant as those obtained by optimizing the wavelength detuning $\Delta\lambda$ and the GO film length L_{GO} .

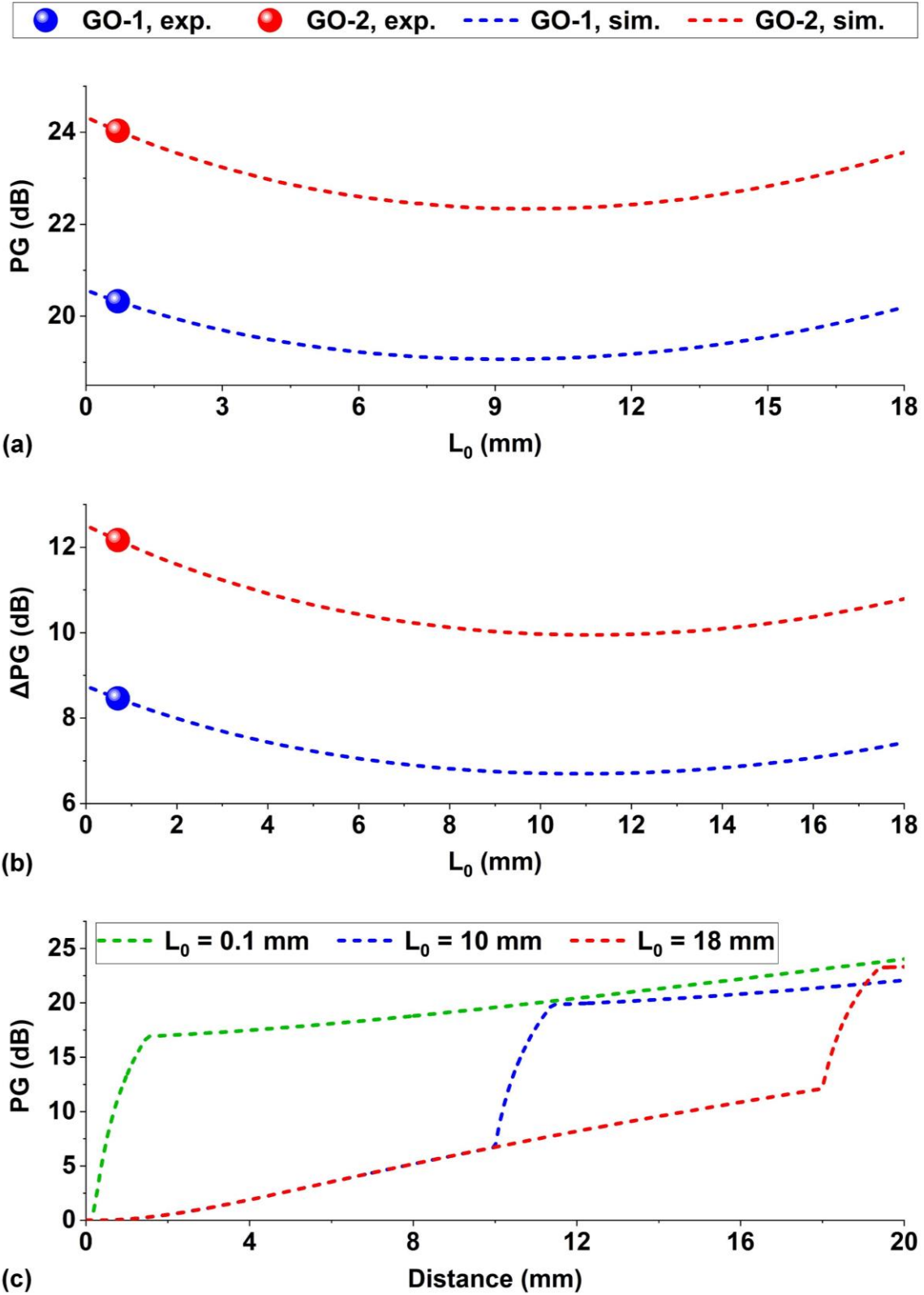


Figure S6. Measured and fit (a) parametric gain PG and (b) parametric gain improvement ΔPG versus GO coating position L_0 . (c) Evolution of PG along the propagation distance for different L_0 . In (a) – (c), the pump peak power, CW signal power, the wavelength detuning, and the GO coating length are $P_{peak} = 180$ W, $P_{signal} = 6$ mW, $\Delta\lambda = -22$ nm, and $L_{GO} = 1.4$ mm, respectively.

VI. Influence of GO's saturable absorption (SA) on the OPA performance

As discussed in **Figure 2d**, the decreased loss induced by the SA in the GO films benefits the OPA performance. In **Figure S6**, we show a quantitative analysis for the influence of the SA on PG and ΔPG of the hybrid waveguides with 1 and 2 layers of GO. In each figure, the solid curve shows the result when considering the SA that induces a slight reduction in loss, whereas the dashed curve shows the result calculated using a constant linear loss of GO, as measured at low CW powers (i.e., the loss in **Figure 2a**). As can be seen, the SA of GO has a positive influence and yields more significant PG and ΔPG for both devices. The impact is more pronounced in the case of the 2-layer device – in agreement with the trend as observed in the decreased loss shown in **Figure 2d**. This suggests that the SA has a stronger influence on the OPA performance of devices with thicker GO films.

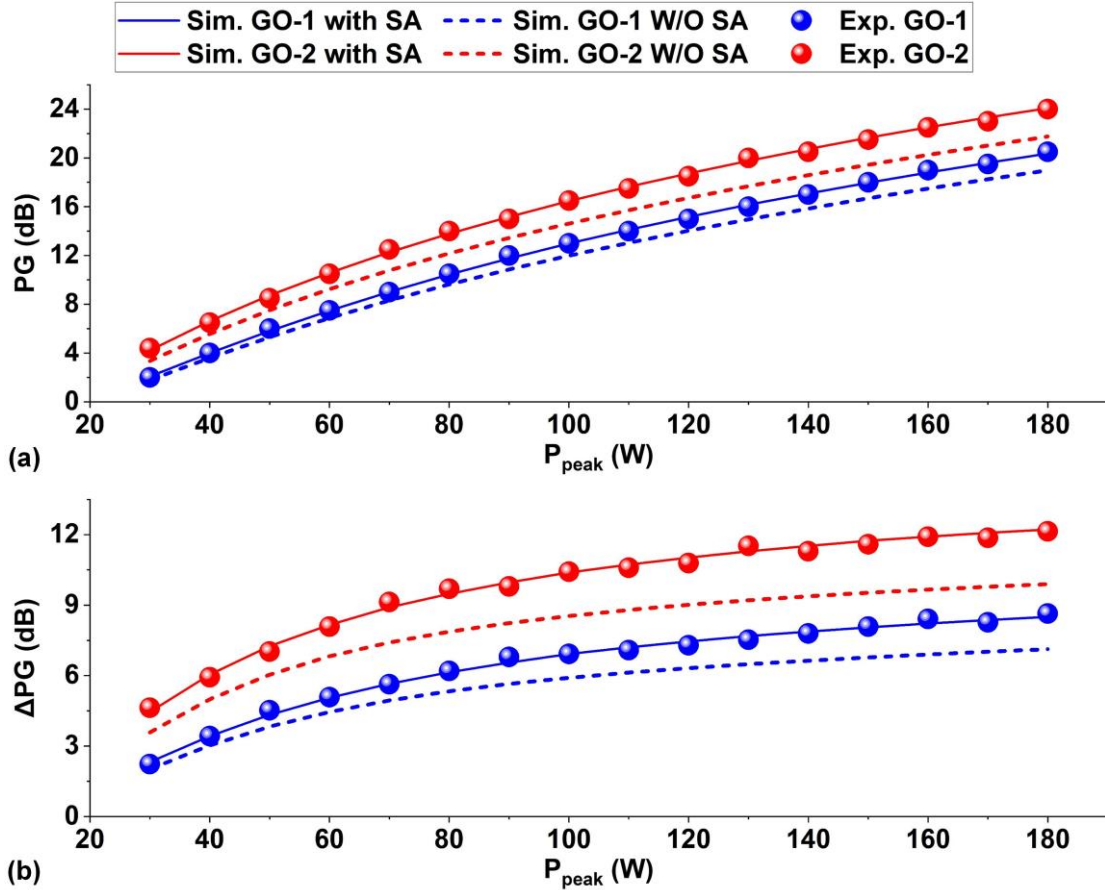


Figure S7. Comparison of (a) parametric gain PG and (b) parametric gain improvement ΔPG for the hybrid waveguides with and without considering the saturable absorption (SA) of GO. In (a) and (b), the solid and dashed curves show the results with and without considering the SA of GO, respectively. The experimental results are shown by data points for comparison. The CW signal power, the wavelength detuning, and the GO film length are $P_{\text{signal}} = 6$ mW, $\Delta\lambda = -22$ nm, and $L_{\text{GO}} = 1.4$ mm, respectively.

References

- [1] P. Demongodin, H. El Dirani, J. Lhuillier, R. Crochemore, M. Kemiche, T. Wood, S. Callard, P. Rojo-Romeo, C. Sciancalepore, C. Grillet, and C. Monat, "Ultrafast saturable absorption dynamics in hybrid graphene/Si₃N₄ waveguides," *APL Photonics*, vol. 4, no. 7, pp. 076102, 2019.
- [2] C. Monat, C. Grillet, M. Collins, A. Clark, J. Schroeder, C. Xiong, J. Li, L. O'Faolain, T. F. Krauss, B. J. Eggleton, and D. J. Moss, "Integrated optical auto-correlator based on third-harmonic generation in a silicon photonic crystal waveguide," *Nat Commun*, vol. 5, pp. 3246, 2014.
- [3] X. Liu, R. M. Osgood, Y. A. Vlasov, and W. M. J. Green, "Mid-infrared optical parametric amplifier using silicon nanophotonic waveguides," *Nature Photonics*, vol. 4, no. 8, pp. 557-560, 2010.
- [4] K. J. Ooi, D. K. Ng, T. Wang, A. K. Chee, S. K. Ng, Q. Wang, L. K. Ang, A. M. Agarwal, L. C. Kimerling, and D. T. Tan, "Pushing the limits of CMOS optical parametric amplifiers with USRN:Si₇N₃ above the two-photon absorption edge," *Nat Commun*, vol. 8, pp. 13878, Jan 4, 2017.
- [5] Y. Qu, J. Wu, Y. Yang, Y. Zhang, Y. Liang, H. El Dirani, R. Crochemore, P. Demongodin, C. Sciancalepore, C. Grillet, C. Monat, B. Jia, and D. J. Moss, "Enhanced Four-Wave Mixing in Silicon Nitride Waveguides Integrated with 2D Layered Graphene Oxide Films," *Advanced Optical Materials*, vol. 8, no. 23, pp. 2001048, 2020/12/01, 2020.
- [6] Y. Zhang, J. Wu, Y. Yang, Y. Qu, H. El Dirani, R. Crochemore, C. Sciancalepore, P. Demongodin, C. Grillet, C. Monat, B. Jia, and D. J. Moss, "Enhanced self-phase modulation in silicon nitride waveguides integrated with 2D graphene oxide films," *IEEE Journal of Selected Topics in Quantum Electronics*, pp. 1-1, 2022.
- [7] Y. Zhang, J. Wu, Y. Yang, Y. Qu, L. Jia, H. E. Dirani, S. Kerdiles, C. Sciancalepore, P. Demongodin, C. Grillet, C. Monat, B. Jia, and D. J. Moss, "Enhanced Supercontinuum Generation in Integrated Waveguides Incorporated with Graphene Oxide Films," *Advanced Materials Technologies*, pp. 2201796, 2023.